FUEL CELL DEVELOPMENT WITH NON-PRECIOUS METAL CATALYSTS

A Thesis

by

BURAK CELAL AYYILDIZ

Submitted to the Office of Graduate and Professional Studies of
Texas A&M University
in partial fulfillment of the requirements for the degree of

MASTER OF SCIENCE

Chair of Committee,	Choongho Yu
Committee Members,	Partha P. Mukherjee
	Arum Han
Head of Department,	Andreas A. Polycarpou

August 2016

Major Subject: Mechanical Engineering

ABSTRACT

Proton exchange membrane (PEM) fuel cells are clean energy sources which are offering solutions to some problems that are caused by climate change and global warming. One of the biggest obstacles in the way of development of PEM fuel cells is the high price of the Pt catalyst; this makes up a large percent of the total cost of the fuel cell. Our research group achieves high fuel cell performance using non-precious, Fe-CNT-PA. This new catalyst can make PEM fuel cells more commercial in future applications. This research tests fuel cell performance using this new catalyst and compares it to the commercial Pt/C catalyst. We propose that Fe-CNT-PA has a good catalytic activity as the PT catalyst. The results of the fuel cell test shows the performance is close to commercial cathode material activity, but more research is necessary to advance the performance of the non-precious catalyst.

DEDICATION

Dedicated to my mother, father and brother

who are always with me with selfless love and have believed in me my whole life.

ACKNOWLEDGEMENTS

I would like to thank my advisor, Dr. Choongho Yu, for his guidance, support and motivation through the entire period of my research. I also would like to thank to my committee members, Dr. Partha P. Mukherjee and Dr. Arum Han.

Thanks also go to everyone at the Nano energy lab, especially Woongchul Choi, Abdullah Tazebay, Jui- Hung Hsu, and Suk Lae Kim for giving advice and helping me to finish my research. Moreover, I would like to thank my roommate Bahadir Basaran and my friends Ahmet Tigli and Bryan Munoz for their support and patience.

I also want to extend my gratitude to the Ministry of National Education of Turkey for financial support during my master degree.

Finally, thanks to my parents and brother for their encouragement, emotional and financial supports.

NOMENCLATURE

Ag	Silver
CPET	Coupled Proton and Electron Transfer
CV	Cyclic Voltammetry
DFT	Density Functional Theory
GHG	Greenhouse Gases
LSV	Linear Sweep Voltammetry
MO	Metal Oxide
MWCNT	Multi Wall Carbon Nanotubes
ORR	Oxygen Reduction Reaction
PEMFC	Proton Exchange Membrane Fuel Cell
Pt	Platinum

TABLE OF CONTENTS

Page

ABSTRACT ii

DEDICATION iii

ACKNOWLEDGEMENTS iv

NOMENCLATURE v

TABLE OF CONTENTS vi

LIST OF FIGURES viii

LIST OF TABLES x

1 MOTIVATION AND INTRODUCTION 1

2 LITERATURE REVIEW 9

2.1 Origin of the Oxygen Reduction Reaction for Fuel Cells 9
2.1.1 ORR at Transition Metals 9
2.1.2 ORR at Non-Precious Metal-Based Catalyst 13
2.2 Non- Precious Metal Catalysts 14

3 CHARACTERIZATION OF THE CATALYST 15

3.1 Imaging the Fe-CNT-PA Catalyst 15
3.2 Electrochemical Characterization of the Fe-CNT-PA Catalyst 18
3.2.1 Sample Preparation for the Electrochemical Measurements 19
3.2.2 Cyclic Voltammetry 20
3.2.3 Linear Sweep Voltammetry 21
3.2.4 Electrochemical Impedance Test 22

4 EXPERIMENTAL SETUP AND PROCEDURE 23

4.1 Catalyst Ink Preparation and Coating the Cathode Electrode 23
4.1.1 Surface Imaging of the Cathode Electrode After Coating 26
4.2 MEA (Membrane Electrode Assembly) Preparation 27
4.2.1 Nafion Pretreatment for the MEA 29
4.3 Fuel Cell Test System 31

5 RESULTS AND DISCUSSION 34

5.1 Electrochemical Test Results 34
5.2 Fuel Cell Test Results 37

6 CONCLUSION AND RECOMMENDATIONS 40

REFERENCES 41

LIST OF FIGURES

Page

Figure 1-1 Representation of a PEM fuel cell redox reaction 3

Figure 2-1 Trends of the activity in ORR as a function of the oxygen binding energy[28] 11

Figure 2-2 Oxygen bonding versus ORR activity (top figure), trends of ORA as parameter of O and OH binding energy (bottom figure) [28] 12

Figure 3-1 TEM images of Fe-CNT-PA 16

Figure 3-2 SEM images of the Fe-CNT-PA and Pt/C. The scale bar for these images is 10 mm for the left column and 4mm for the right one.[43] 17

Figure 3-3 Cell setup for electrochemical testing 18

Figure 3-4 Glassy carbon linked with coated carbon paper 19

Figure 3-5 CV analysis of the Pt catalyst at PEM fuel cell [44] 21

Figure 3-6 Eq. circuit showing a fuel cell[45] 22

Figure 4-1 Fe-CNT-PA catalyst slurry 24

Figure 4-2 Various coating methods of the catalyst (Fe-CNT-PA), (a) rolling (b) dipping (c) syringe (d) spray gun 25

Figure 4-3 Coating method of the catalyst (Fe-CNT-PA), drop coating 26

Figure 4-4 Optical microscope set-up with polarizer and analyzer lenses 26

Figure 4-5 Surface morphology of different types of cooling ambient 27

Figure 4-6 Surface morphology of the commercial Pt/C cathode material 27

Figure 4-7 MEA assembly 28

Figure 4-8 MEA the thickness of the electrodes and Nafion. 29

Figure 4-9 Nafion 117 pretreatment steps 30

Figure 4-10 MEA and PEM fuel cell configuration 31

Figure 4-11 Schematic illustration of the fuel cell test system 32

Figure 4-12 Single-stack PEM fuel cell test system 33

Figure 5-1 Cyclic voltammetry performances in 0.5 mole H_2SO_4.....34

Figure 5-2 ORR performance of the samples above in 0.5 M H2SO4 at 1600 rpm 35

Figure 5-3 The EIS spectrum at of the catalyst coated fuel cell equivalent circuit in the Nyquist form. The angular frequency varies from 0.07 to $5x10^5$ rad/s. 36

Figure 5-4 I/V curves at 80^OC for the fuel cell where the red line is commercial Pt/C, the blue line is Fe-CNT-PA with MWC that is compared with Science, 2011. 332(6028): p. 443-447 [23] the dark blue line is PANI-FeCo-C, the yellow line is PANI-C and the grey line is PANI-Co-C.....38

LIST OF TABLES

Page

Table 1 Parameter of the fuel cell test system.....32

Table 2 Elemental composition of the Fe-CNT-PA and Pt/C catalyst for RDE test 36

1 MOTIVATION AND INTRODUCTION

Nowadays, climate changes and global warming cause numerous changes that affect our life. The irreversible risks and ruinous outcomes of the global warning have been concerned politicians and scientists to prevent harmful effects of it. To see the signs of the global warning, the average temperature of the twentieth-century all over the ocean and land surfaces was $0.9^{o}C$ lower the September 2015[1]. From the Intergovernmental Panel on Climate Change (IPCC) forecasting, temperature of the world will be increased $2^{o}C$ at the current rates of the CO_2 distribution level by the 2100. This amount of the rise may cause numerous harmful effects at the climate of the Earth[2]. To stay the $2^{o}C$ range, rate of the greenhouse gases (GHG) should be lower than 31-44 gigatonnes of the CO_2 by 2030[3]. The high percentage of the greenhouse gas emissions is obtained by the transportation sectors and electricity power plants. One third of the energy usage that is 45000 TWh of the usable energy[4], uses up by the transportation sectors per year[5]. Mainly fossil fuels uses to meet up this much amount of the demand and, especially at the transportation area the demand is much more dependent to fossil fuels. In the main energy source is, the all areas included, the fossil fuels which is the one of the primarily source of the global warming. For this reason we should shift the fossil fuels to environmental friendly energy sources to keep the trend of the GHG at a certain lever. To solve the primarily requirement of electrical vehicles and

different types of the source of the energy, it is mostly recommend to utilize the fuel cells and batteries[6, 7].

A fuel cell creates DC electricity from the chemical energy of the fuel via the redox reaction at the anode, release the electron to the external circuit, and cathode that get electrons from the external circuit. Briefly, it is an electrochemical energy converter. In 1839, Sir William Grove who is the pioneer of the fuel cell, discovers the general theory of the energy conversion[8]. This discovery stays a scientific curiosity since the production fuel cell whose capacity is 6 kW by Francis T. Bacon in the late 1950s. Moreover, N.A.S.A used the PEM fuel cell at the Germini and Apollo Space Programs to produce energy for the basics life necessaries for the astronauts. Willard Thomas Grubb from the General Electric (GE) created the first one and regenerated with platinum as catalyst on the cathode by Leonard Niedrach. In 1993, fuel cell exampled with bus by the Ballard Power Systems. The first passenger car, Green Car, used the fuel cell as an energy source[9]. Last decade, due to high impact of the global warning, companies and the governments are funding the research about the fuel cells. These researches are focused on making the operation performance better and reduce the cost of the MEA to make the fuel cell competitive with the fossil fuels. In the middle of the 2000s, CUTE project in Europe demonstrate fuel cell buses from Australia, Europe and China. Due to low emission ratio, high combustion efficiency and easy to refueling processes, it shows possible investments at this area by companies. Over the last decade, fuel cell applications are not only increase at the transportation but also various applications like portable educational fuel cells for teaching the basics of the

electrochemical systems. Moreover it uses at some factories that consume their energy from fuel cells up to 40-kW. All these developments at this area force the governments to invest it due to possible job creation and economic advantages.

Fuel cells are electrochemical units that generate electricity via redox reaction at anode and cathode. During the oxidation reaction, the protons unleash and transfer to cathode. Because of the non-electrical conductivity of the membrane, electrons disengage from the hydrogen flow go through the electrical detour fulfill and that generate the DC electricity. This reaction represented at the below figure.

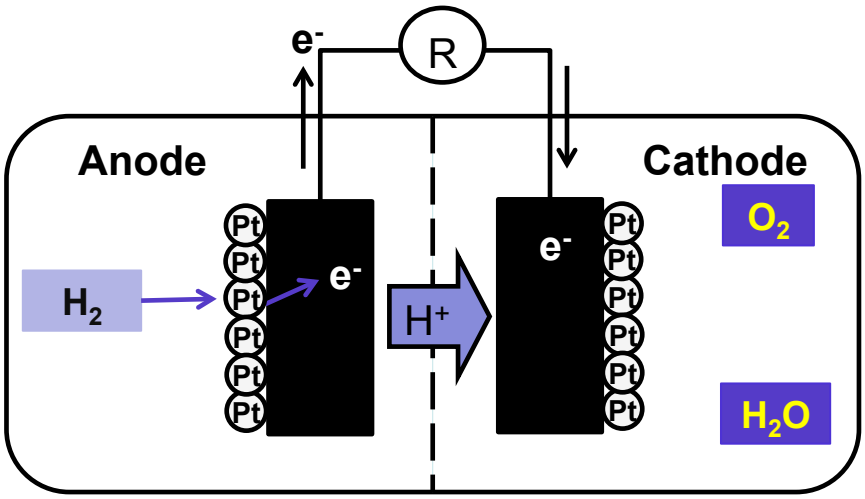

Figure 1-1 Representation of a PEM fuel cell redox reaction

Fuel cells named by using kind of the electrolyte, namely

- Alkaline fuel cell (AFC) is the most electrical efficient fuel cells however; it is only the case of the pure gases that is also its major disadvantage in practical use.

The KOH electrolyte with 85-wt% is used for high temperature and 30-35 wt% used for the lower temperature applications. The main reason make it more affective system is ORR kinetics is faster in alkaline solution rather than acid. One drawback of this fuel cell is low tolerance to CO_2.

- Proton exchange membrane fuel cell (PEMFC) uses a very thin proton conductive polymer membrane, like perfluorosulfonated polymer, as an electrolyte. It operate at lower temperature, typically 60-80^{o}C, were used at NASA missions at first. Due to low kinetic speed, platinum uses as a catalyst to advance the kinetics of the system. The most important development at these cells is the using of the Nafion membranes, which are more stable than the polystyrene sulfonate one. It is promising area of the future of automobile industry and small-scale power generation, and portable devices[10].
- Direct methanol fuel cells (DMFC) are mainly similar to PEMFC that uses different fuel, methanol, rather than hydrogen as source of the fuel. Due to methanol can easily get from numerous kind of resources, natural gas, biomass, etc., and high specific density of energy, it is favorable to low temperature applications. Very few alcohols can consume directly as a fuel in fuel cells and one of them is the methanol. Furthermore, it can be consumed electrochemically. The concentration of the liquid methanol at the anode is important to achieve the fraction of the fuel. Therefore, the devices called methanol sensors which measure current are curial to operate the DMFC[11].

- Solid oxide fuel cells (SOFC) use nonporous MO (metal oxide) as electrolyte. Its operation temperature is high, 800 – 1000^{o}C, where it hard to find appropriate materials that have thermal and chemical stability at high temperature. Moreover, due to the solid electrolyte, there is no leakage problem, which can be seen at liquid electrolyte fuel cells. This type of the cell is an also well water management cell due to the straightforward solid-gas system.
- Molten carbonate fuel cell (MCFC) has the molten carbonate that is the composition of electrolyte combination of Li, K and Na, which can enhance with Al_2O_3 fibers that improve the mechanical properties of the fuel cell. One of the biggest advantages of the MCFS is the operation temperature that is between 600 to 700^{o}C where the ionic conductivity is higher and less precious catalyst need to operate the fuel cell. The efficiency of the MCFC can reach up to 70% depends on the operation temperature when other power generations are used with it[12].
- Phosphoric acid fuel cells (PAFC) use precious metal (Platinum) catalyst to its anode and cathode due to low operation temperature that is between 150 and 200^{o}C and the electrolyte material is concentrated phosphoric acid.

Oxygen reduction reaction (ORR) is the main electrochemical reaction for conversion of the electrochemical energy at fuel cells[13]. Nevertheless, its sluggish ORR kinetics due to O=O bond activation/ cleavage and three different phases of the reaction restrict our control mechanism of the performance. The slow kinetics of ORR require huge amount of loading of precious metal catalyst, Pt- based catalyst, that is unfavorably accompanied by the increased cost of the fuel cell. Moreover, Pt-based catalyst gives the great in terms

of stability and also low over potential[14]. From the date of the DOE, United States Department of Energy, the cost ration of the Pt-based catalyst to all over the fuel cell stack is 56% that is the project cost[15, 16]. Hence the high ratio of the cost of the fuel cell depends on the Pt-based catalyst, reduction of the cost linked to catalyst directly. Due to stability and advanced ORR electrochemistry are primarily obstacles; testing vehicles use 0.4mg per square centimeter of more on the cathode for mass production. Over the past decades, numerous searches try to reduce cost of the making stack fuel cell by decreasing amount of the Pt-catalyst or even new materials as catalyst without losing any performance or durability of the fuel cell. From the advanced material science and nanotechnology, there is major improvement in designing and synthesis of Pt-based or non-precious metal catalyst over the past decades[17-19]. This chapter gives a brief background and motivation into why non precious metal catalyst is important to development of the next generation of fuel cell.

Among the numerous non-precious metal catalyst, metal-nitrogen complexes on the carbon base materials are the best candidates because of the reduced price, high stability and activity[20-23]. However, it has suffered from several problems which are active sites anion bonding or weak performance of the nitrogen in acidic environment[24]. There are several theories about the effect of the transition metal in carbonaceous material doped with nitrogen. On the one hand, transition metal involves the ORR by transferring electron from electrode to oxygen[25]. On the other hand, transition metals only help to create nitrogen doped carbon nanostructures while process of the nitrogen incorporation. At this theory, it is assumed it is not the participant of the

reaction or assists the electron transfer[26]. In this thesis, I use the catalyst which is designed by our group, new nitrogen doped carbon nanotube based catalyst with iron that is promising a new catalyst which can be replace with Pt-based catalyst.

All aforementioned advancing catalysts make the fuel cells more promising energy source for next generation. There are several properties make the non-precious metal catalyst attractive to research. They offer numerous benefits:

1. High Efficiency- due to efficiency of the fuel cell is higher than the efficiency of the traditional engines, fuel cells promises more investment for automotive industry. Moreover, its efficiency is also higher than the power plants, so fuel cells are attractive for power generation.
2. Zero emission- Due to fuel of the PEM fuel cells is hydrogen; it generates zero emission after the chemical reactions. Even though the exhaust products are water and unused air, there is no direct hydrogen source that use as available fuel. While generating the hydrogen as fuel, there is also some emissions are generated but the amount of emission is too low when we compare the ratio of the conventional energy transfer systems.
3. Promise to low cost- the mechanism of the fuel is simple and there are no moving parts, hence the possibility to mass production is extremely high. Especially at the automobile applications, due to low cost of our new catalyst it is more comparable to traditional power sources. Due to promising developments of the fuel cell's catalyst mass production techniques are still developing.

4. Quiet-Due to no moving parts and the noise free chemical reactions, they are inherently soundless. It is an important feature for various kinds of applications for instance military applications, portable power sources and power stations for back up.
5. Size and weight- there are several types of fuel cells depends on their kind of applications that changes between microwatts to megawatts. When we compare the size and weight of the energy source of the automobile. Fuel cells are more effective than the traditional combustion engines thus it suggest advantage over the competing the developments on this industry.

2 LITERATURE REVIEW

2.1 Origin of the Oxygen Reduction Reaction for Fuel Cells

The origin of the Oxygen reduction reaction (ORR) is still not clear due to its complex sluggish kinetic. It occurs at the cathode and the catalyst material for has to be stable under the harsh conditions but also, chemically active to reduce the oxygen. Furthermore, it has to be noble for effortlessly remove the water from the surface of the catalyst. It is critical to complete the reaction at catalytic site.

2.1.1 ORR at Transition Metals

For transition metal catalyst two-electron reduction is more common at less active metals and four-electron reduction is common at highly active transition metals, such as Pt. At the ORR, There are three hurdles steps whose are electron transfer of the first electron at ORR, desorption of the environment and hydration of oxygen.

At the proton exchange membrane fuel cell (PEMFC, cathode electrode is the main reason of the voltage losses due to its sluggish kinetics. In the acidic media, there are two main paths of the ORR[27]. On the first path, four-electron transfer caused the water formation. Firstly, metal surface adsorbs O_2 and O=O bond is broke that gives O* (adsorbed oxygen). These atoms are protonated by the H^+ that come across from the anode side of the PEM and reduced to OH* (hydroxyl). Herein, OH* is more protonated

and reduced to produce water that is going to leave the surface of the catalyst[28]. The first path can be shown like:

$$\tfrac{1}{2}\, O_2 + * \rightarrow O*$$

$$O* + H^+ + e^- \rightarrow OH*$$

$$OH* + H^+ + e^- \rightarrow H_2O + *$$

$$O_2 + 4H^+ + 4e^- \rightarrow H_2O \text{ (overall reaction)}$$

On the second path, it is the case of the bonding of the O=O bonds do not break while the O2 adsorption. In this way, two-electron reduction is observed even though the mechanism is not clear. After this reaction H_2O_2, which is undesirable, is produced [28]. Hydrogen peroxide is mostly undesirable because it degrades the membrane of electrolyte.

$$O_2 + * \rightarrow O_2*$$

$$O_2* + H^+ + e^- \rightarrow HO_2*$$

$$HO_2* + H^+ + e^- \rightarrow H_2O_2*$$

$$H_2O_2* \rightarrow H_2O_2 + *$$

$$O_2 + 2H^+ + 2e^- \rightarrow H_2O_2 \text{ (overall reaction)}$$

Through the amount of the H_2O_2, the activity of the catalyst can be determined[29]. One of the criteria of a good catalyst is the amount of the hydrogen peroxide should be low. However the kinetics of the ORR and HOR are not similar, reaction rate trends are similar at different electrodes. Activity of the catalyst should be

strong enough to aid a reaction but not too strong which causes block of the activity. In the case of binding interaction is not too strong, the substrate cannot adsorb well on the catalyst itself. Herein, there may be slow reaction or may not take the place. Additionally, if the binding energy is further powerful, the surface of the catalyst will be baffled by product and activity of the catalyst will end. From the Sabatier principles [30] illustrated the relationship between substrate and catalyst. Recently, Norskov et al. using density functional theory (DFT) to calculate the free energy of the all agents as function of the potential of the electrodes [28, 31, 32]. These results are depicted by Balandin's volcano that shows the activity of the catalyst versus adsorption energy for the ORR.

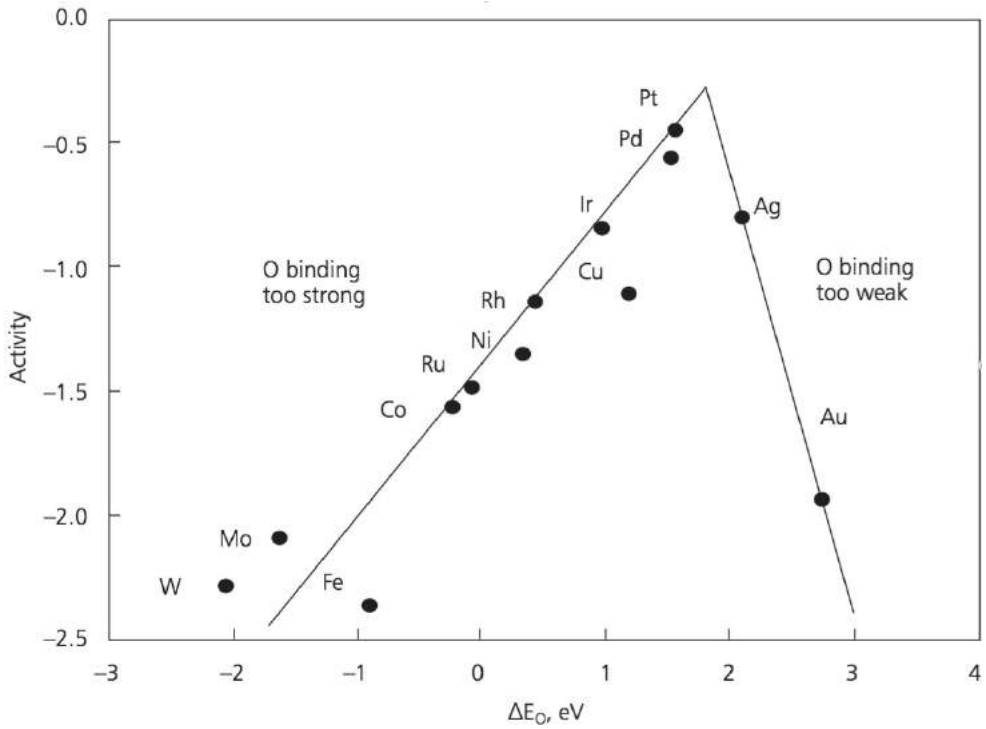

Figure 2-1 Trends of the activity in ORR as a function of the oxygen binding energy[28]

Figure 2-1 depicts various metals and O atoms binding energy versus oxygen reduction activity. From this plot, Pt is the best candidate to be catalyst by its high theoretical activity peak from the DFT calculations. Through the aforementioned steps of the ORR, there are two steps need catalyst more to activation. First bind O then, bind the OH. Herein, figure 2-2 is illustrated Pt is the best metal catalyst that is close the optimal binding energy at the activity against not only for O but also OH binding energies.

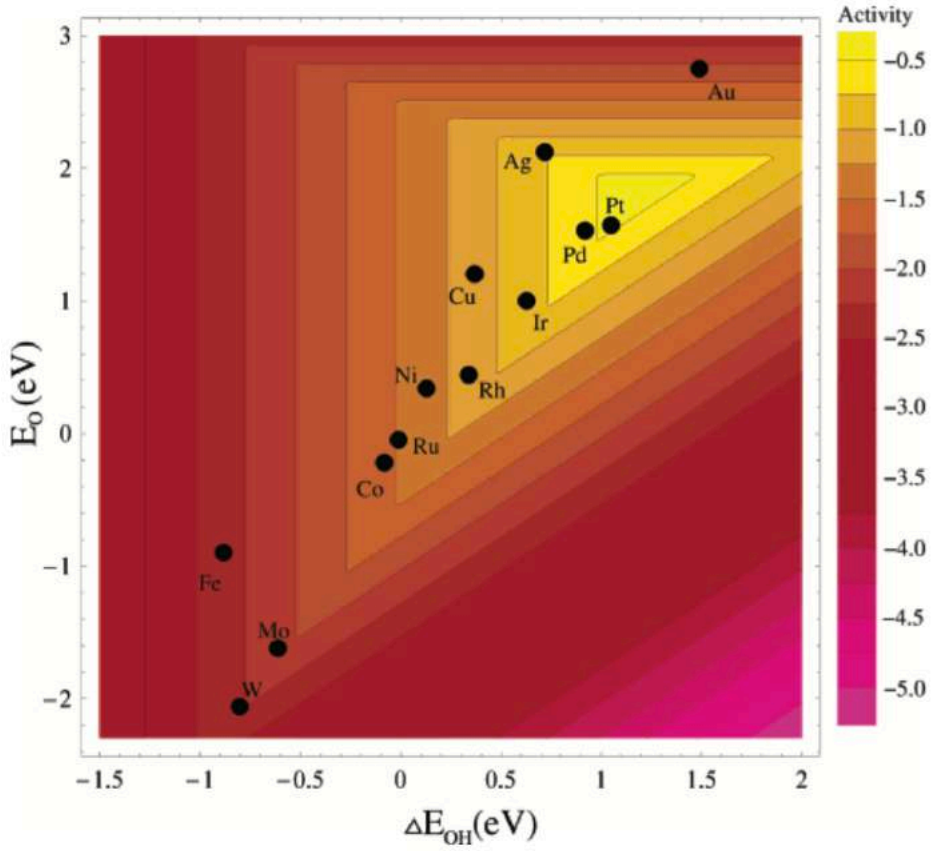

Figure 2-2 Oxygen bonding versus ORR activity (top figure), trends of ORA as parameter of O and OH binding energy (bottom figure) [28]

2.1.2 ORR at Non-Precious Metal-Based Catalyst

Non-precious metal catalysts are getting more popular by the recent push for the mass production of the various energy sources. The most promising catalyst for the ORR is transition metal (Fe, Ni, Co. etc.)-Nitrogen-carbon materials, which are abundant at the nature. Since Jasinski et al. figured out the metal phthalocyanines featuring an MN_x center are able to be catalyst in ORR under acidic ambient there is an encouraging improving at M-N-C types of electro catalysts as catalyst at ORR[33]. However, mechanism of the M-N-C catalysts is still not clear. There are several theories about what part of M-N-C catalysts are the active side of it. One of them is, MN_x will not be the only active side. The carbon black that delivered during the heat treatment, is one of the high catalytic active side[34]. On the other hand, many others proposed metal sites of the MN_x are not a part active part of the catalyst structure, but it centers catalyze the pyridinic and pyrrolic nitrogen[35]. The one method to use metal to catalyze the catalytic layer is creating special catalyst architecture by growing the carbon nanostructure rather than using the metal as catalyst. Specific structure of the carbon is created at the edge planes, which cause higher amount of the pyridinic nitrogen at the catalyst. The possible role of the Fe is that helps growth of the CNT with higher percentage of the catalyst surface, whether the forerunner, which is pyrolyzed in an organic macro-cycle and or CN_x species[36-38]. From these different approaches, it is elusive conclusion if the pyridinic nitrogen played the direct role in the ORR or its role

is more indirect nature by advancing the electron donation ability of the carbon basis structure.

2.2 Non- Precious Metal Catalysts

Due to low cost, high durability and activity, M-N-C composition catalysts are the most popular through the numerous non-precious metal catalysts[21]. Small organic molecules such as acetonitrile or pyrrole[39], PANI, inorganic metal sources like ammonia gas [25] and metal-N_4 [40] are generally used as N source. Researches state catalyst delivered by polyaniline are more reactive to ORR[41]. Moreover, Zelenay group use PA-Fe-C and Pa-Co-C catalysts to compare which is more active in ORR. The results show best performance can achieve from their combination that is mixed-transition metal catalyst[23].

Yu group develop new catalyst whose base material is randomly rotated nitrogen doped-CNT sponge with various types of nitrogen with Fe as a metal component by the way to produce it massively. It shows good performance while compare it to commercial precious metal catalyst. This group claimed the high performance of the catalyst due to its porous structure[42].

3 CHARACTERIZATION OF THE CATALYST

3.1 Imaging the Fe-CNT-PA Catalyst

Scanning electron microscope (SEM) and transmission electron microscope (TEM) are using for exploring surface architecture of Fe-CNT-PA and getting high quality images of the Fe-CNT-PA surface at high quality.

At TEM Fe-CNT-PA used to research the amounts of the graphitic lines and the distribution of these lines. Small amount of the sponge is put in a solvent. Ethanol was used as a solvent, which dries quickly. Sonication of solution for few seconds is used to disperse particles well. Then 1 microgram of the solution is dropped to the carbon grid. TEM images were obtained with JEOL JEM-2010 TEM with 200 kV accelerating voltage and LaB_6 filament. Gatan SC1000 ORIUS CCD camera (Model 832) was used to attain images. Interlayers distance between the graphitic lines that is 0.34nm, were measured to calculate the calibration. All TEM samples were mounted on a non-tilted sample holder.

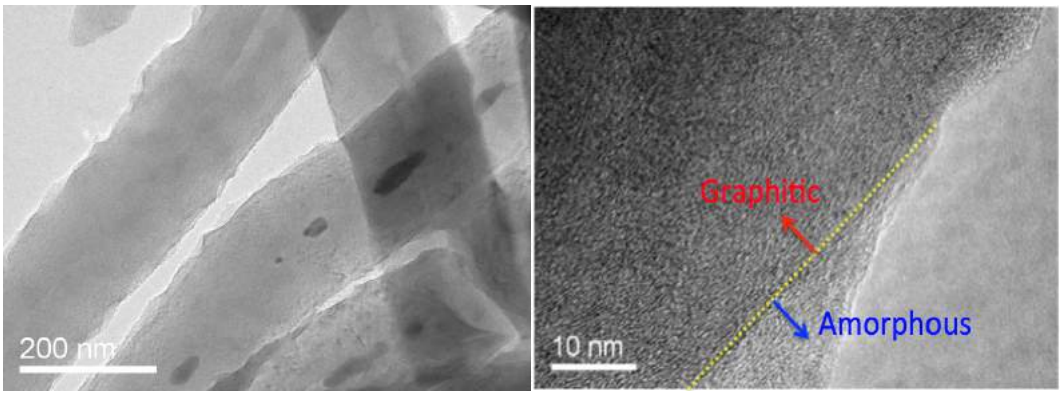

Figure 3-1 TEM images of Fe-CNT-PA

Transmission electron microscope images show that there are several graphitic layers are on the CNT walls. Also, amorphous layers, which created due to the polyaniline coating, can be seen. From the lower magnification images, diameter of the multi-wall carbon nanotubes is approximately 190nm,and the distance of the two graphitic layers is 0.34nm.

A scanning electron microscope (SEM) image obtained by JEOL JSM-7500F shows high porous structure of the catalyst with comparison the commercial Pt/C catalyst at figure 3-2.

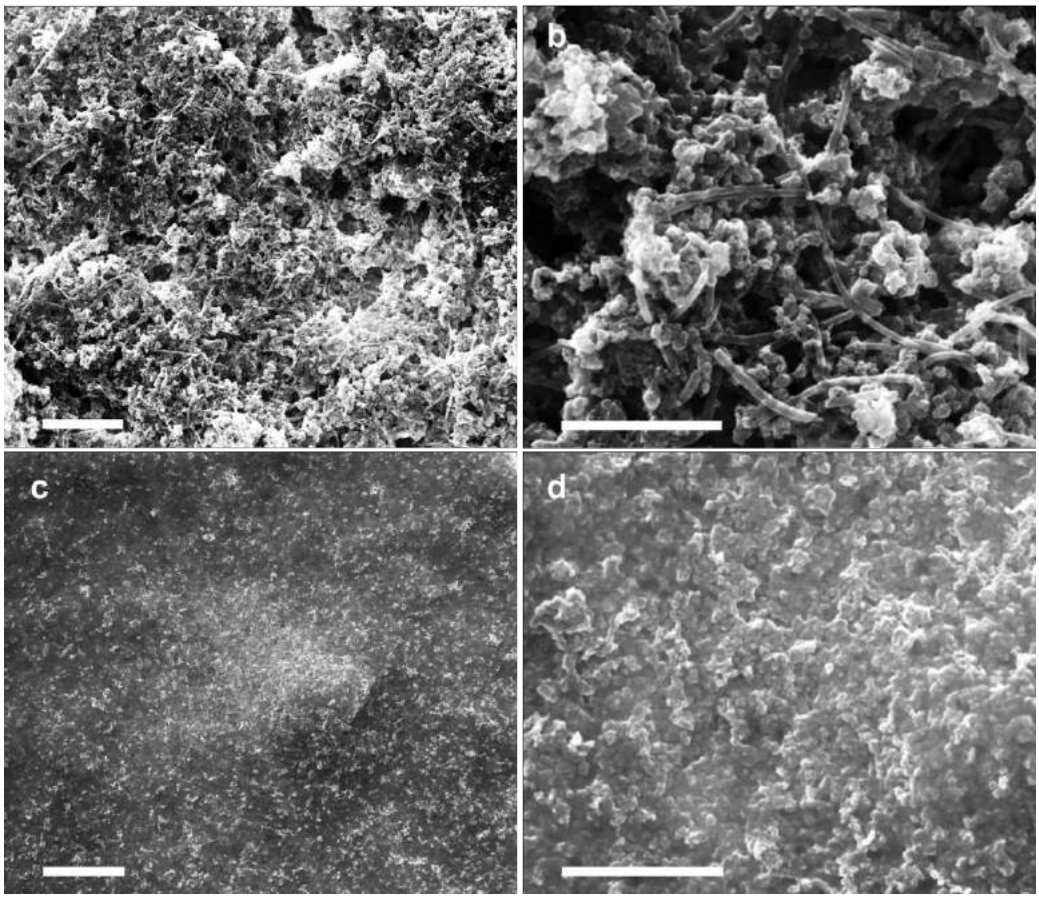

Figure 3-2 SEM images of the Fe-CNT-PA and Pt/C. The scale bar for these images is 10 mm for the left column and 4mm for the right one.[43]

3.2 Electrochemical Characterization of the Fe-CNT-PA Catalyst

Cyclic voltammetry (CV) and rotating disk electrode (RDE) are standardized techniques for characterization of the catalyst in case of catalytic activity at the ORR. Thus, this part focused on the two experiments with different types of inks and conditions.

Figure 3-3 shows cell set up for CV and RDE electrochemical analysis. It is designed there electrode, reference, counter and working electrodes, glass cell. The electrolyte is O_2 saturated that takes 30 minutes (before the test) with 100sccm in 200 mL of 0.5 M H_2SO_4. During the electrochemical measurements, O_2 is keeping to feed to the electrolyte to support O_2 saturation while obtaining the results of the electrochemical tests.

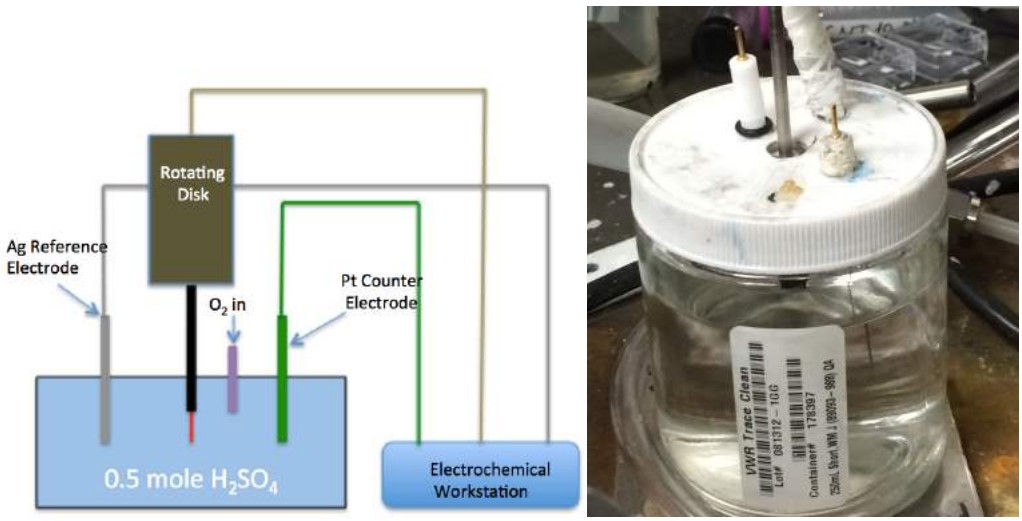

Figure 3-3 Cell setup for electrochemical testing

3.2.1 Sample Preparation for the Electrochemical Measurements

Samples were obtained ink for to measure their electrochemical catalyst activities. To achieve homogeneous ink, a 7 mg catalyst and 160 µL Nafion solution (5 wt%, Fuel Cell Earth) were dissolve in DI water and ethanol, EMD Millipore (%80-%20) by pen-type sonication for 30 minutes. Electrochemical tests used an electrochemical workstation (CHI 640D, CH Instruments). From figure 3-3, three-electrode system using a platinum wire as a counter electrode and Ag/AgCl as a reference electrode. 5 µL of catalyst ink has been dropped on the glassy carbon electrode, working electrode. Furthermore, same amount of the Pt/C catalyst ink prepared as the same method to compare results. After dropping, 0.5 mg cm^{-2} catalyst loaded on the glassy carbon whose diameter is 3 mm.

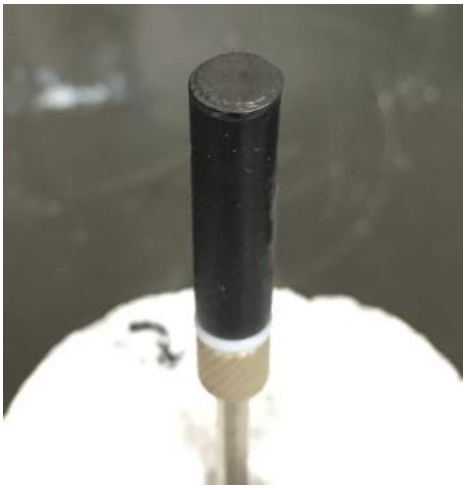

Figure 3-4 Glassy carbon linked with coated carbon paper

3.2.2 Cyclic Voltammetry

Cyclic voltammetry is the one way to get information about the catalytic activity of the catalyst in the ORR. This method considers of cycling of the potential between chosen upper and higher points and saving the current. These interspaces are chosen by the interest of the thermodynamic potentials of the reaction if interest that is ORR in my research. The definition of the voltammetry is the resulting current density versus potential. The peak potential and the peak current density can derive the catalyst activity.

Figure 3-4 shows a typical CV of the oxygen reduction reaction on the commercial Pt catalyst. At this figure potential window range is between -0.3 and 1.2V. As seen at the figure, oxidation happens at increasing potential and reduction at the decreasing potentials. On the one hand, all along Pt catalyst surface absorbs the hydrogen atoms at oxidation, hydrogen atoms get off and transfer of the H atoms through the electrolyte. On the other hand, while potential decreases, Pt oxides reduce to Pt that is the proof of the reduction peak at CV. This peak is directly related with ORR. From the degree of the potential and absolute value of the peak we can indicate the catalytic activity of the sample.

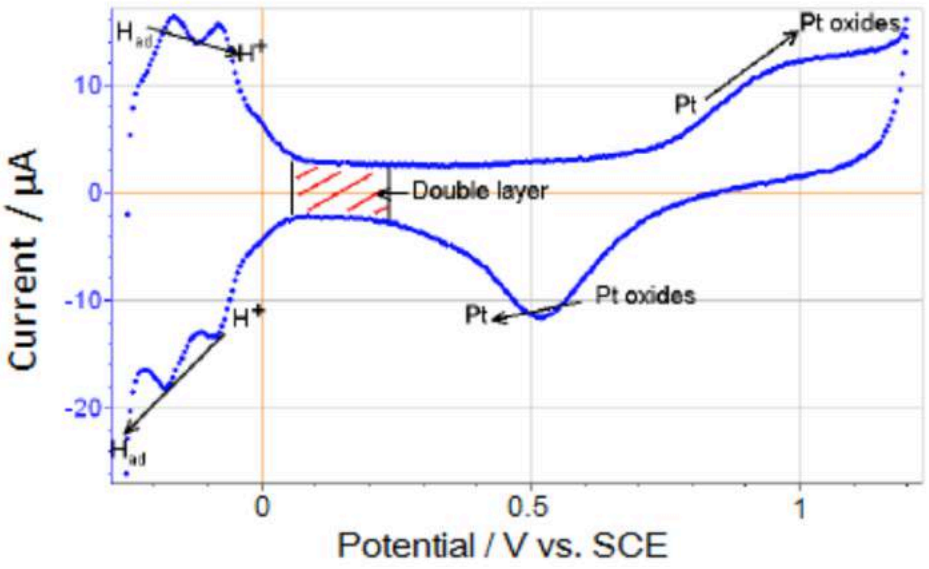

Figure 3-5 CV analysis of the Pt catalyst at PEM fuel cell [44]

3.2.3 Linear Sweep Voltammetry

In linear sweep voltammetry (LSV), voltage of the cell is glide only in one way; therefore it is similar to half of the CV. To get the diffusing limited current LSV is measured at a relatively slow sweep ratio that is not dependent on the potential. These properties of the rotating disk electrode make it one of the most popular methods of characterization of the kinetic feature of the catalyst. RDE controls the convective diffusion, which is defined as the moving species because of the external forces. At this experiment, convection can control by the speed of the rotation of the electrode. By controlling the convection, density of current is up to 100 times greater than steady state diffusion restricted value.

3.2.4 Electrochemical Impedance Test

Electrochemical impedance spectroscopy allows measurement of the process occurring with numerous time scales, like as charge transfer, ion conduction, mass transport and double layer charging. Essentially, it is a measure of the ability of the system to impede electrical current. Current signal, whose frequency and amplitude are known, is applied to measure the amplitude and frequency of the resulting signal. Several equivalent circuits models (resistor, capacitor, inductor, etc.) are needed to convolute the final impedance spectra and data, which we are looking for.

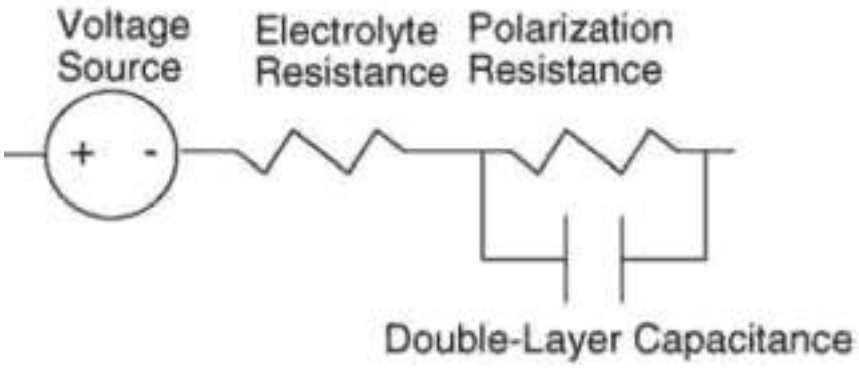

Figure 3-6 Eq. circuit showing a fuel cell[45]

Figure 3-6 is depicted, where R_{ct} is charge transfer resistance, R_e is both ionic and electronic resistance, C is the capacity and Z_W is Warburg impedance, which is accounting for mass transportation.

4 EXPERIMENTAL SETUP AND PROCEDURE

4.1 Catalyst Ink Preparation and Coating the Cathode Electrode

DI water based ink was prepared by 50 mg catalyst, 8.3 mg MWC and 24.9 mg solid Nafion solution (5 wt%, Fuel Cell Earth) were dissolve in DI water and IPA, by pen and bath type sonication for 3 hours and over night, respectively. The weight of the catalyst and amount of the 5% Nafion to the catalyst were calculated using:

$m_{catalyst} = A_{cathode} * G_{cat}$

$$m_{5\%NF} = \frac{100\%}{w_{NF}} * m_{catalyst}$$

where $m_{catalyst}$ is the weight of catalyst for the ink, $A_{cathode}$ is the membrane surface area, G_{cat} catalyst loading amount on the paper and $m_{5\%NF}$ is the amount of five-weight percentage of Nafion solution.

The weight of the catalyst is calculated depends on the loading weight that is 5 to 10 mg/cm^2. From the RDE results of several samples, using MWC will improve the electrical conductivity therefore 10% of the total amount of the ink of the MWC (Outer diameter: 8-15 nm; length: 10-50 um) is added.

Figure 4-1 depicted homogenous mixture of the slurry after pen and bath type sonication for 3 hours and over night, respectively.

Figure 4-1 Fe-CNT-PA catalyst slurry

Catalysts were coated onto the surface of the 5cm^2 area GDLs by several methods, which are dipping, syringe, rolling, spray gun and drop casting. Figure 4-2 shows these methods from (a) to (d). At the rolling method, a square piece of glass is used as base and use tape on the edges of the glass to create the cavity that can determine the catalyst layer thickness. This method is not a good option due to fluidal feature of the ink and there is a huge amount of catalyst is attached on the roller. At the (b), dipping method, the 3 mm^2 and 130 mm thick sponge dip to the catalyst ink in 30 minutes. After this time period, it puts on the heater to dry it up. It is an effective way to load the catalyst however; making the MEA is the biggest problem at this method due to brittle feature of the cathode electrode after drying. The third method (c) is also use same size of the sponge to syringe the catalyst in the sponge but it is not an effective way to deposit the ink because dried ink stuck at the needle after a while. The other way of the loading of the catalyst is the spraying the catalyst ink on the GDL. Unfortunately, only 1/5 of the catalyst is attached the GDL that amount is pretty low to reach the high

amount of the loading rates. It is caused by the spray gun and process itself. It can be improved by a better spray gun. The last method is the dropping the catalyst on the carbon paper and heater can be use to get faster results.

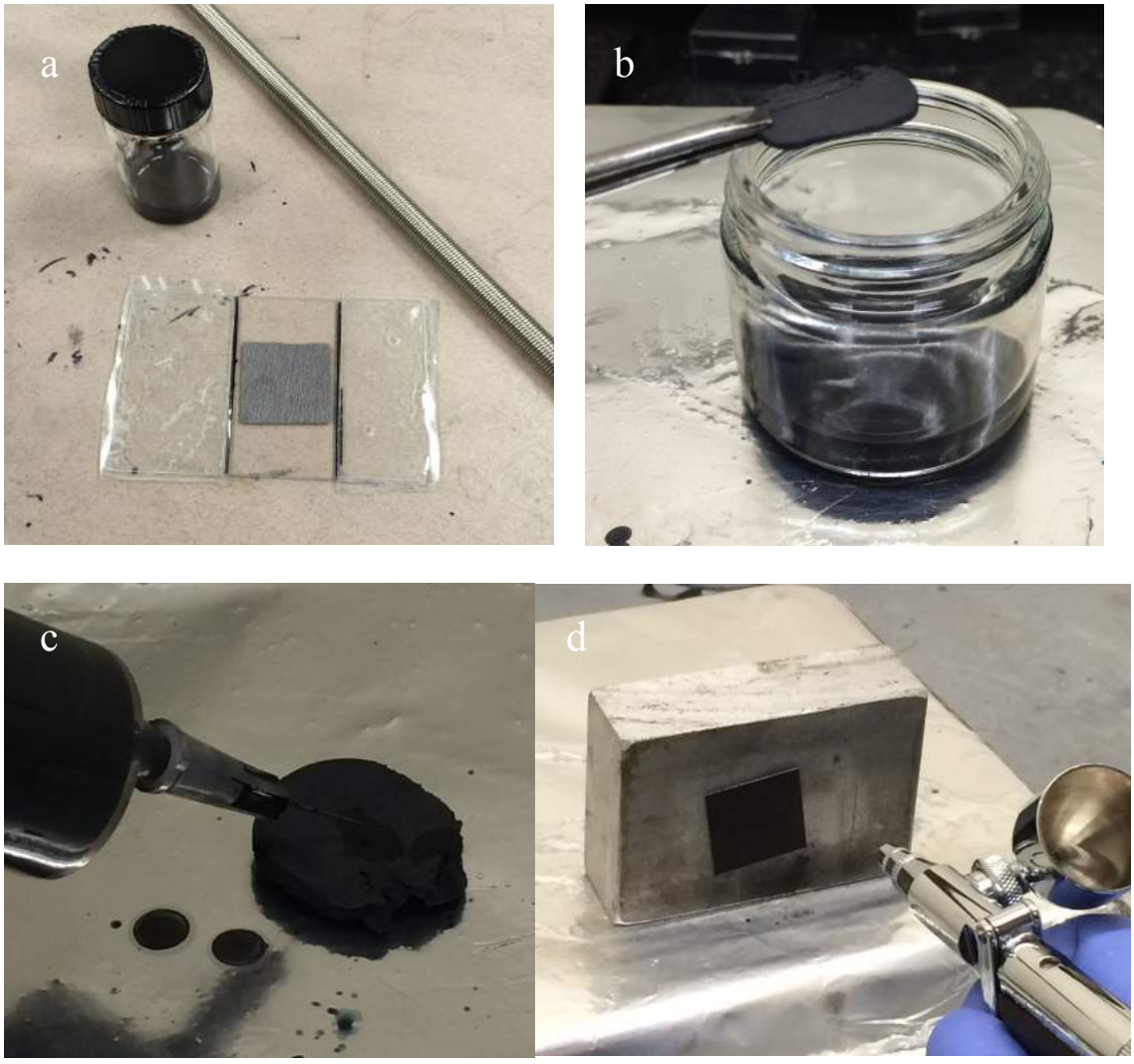

Figure 4-2 Various coating methods of the catalyst (Fe-CNT-PA), (a) rolling (b) dipping (c) syringe (d) spray gun

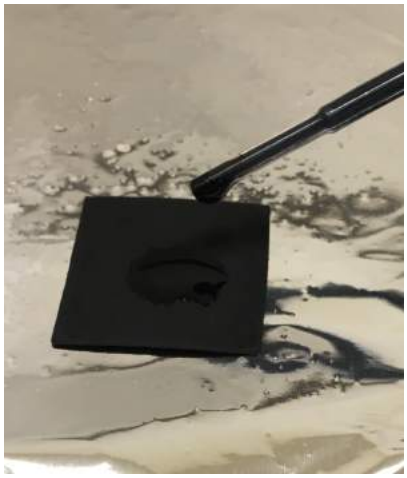

Figure 4-3 Coating method of the catalyst (Fe-CNT-PA), drop coating

4.1.1 Surface Imaging of the Cathode Electrode After Coating

One of the performance parameters of the fuel cell test system is the surface morphology of the cathode, which wills causes the voltage loses due to improper surface condition.

Figure 4-4 Optical microscope set-up with polarizer and analyzer lenses

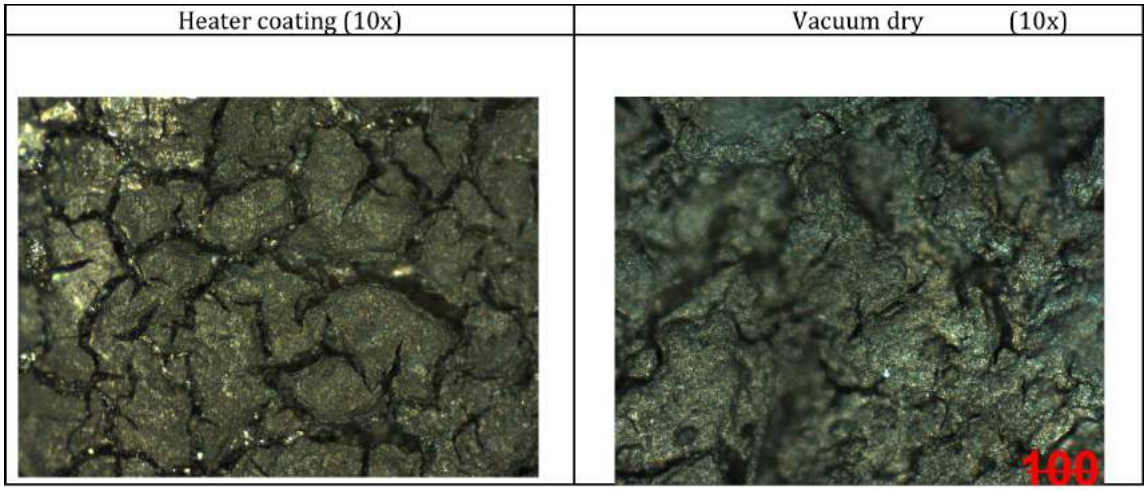

Figure 4-5 Surface morphology of different types of cooling ambient

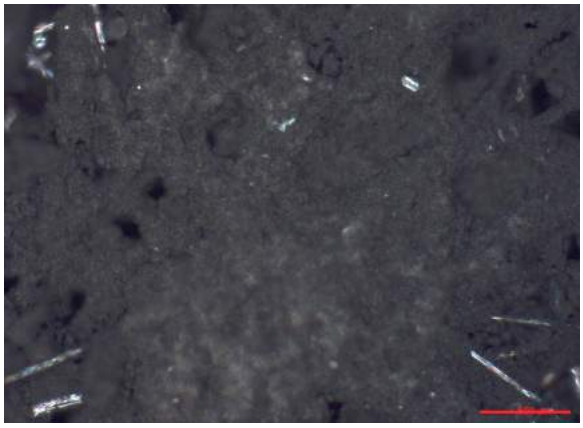

Figure 4-6 Surface morphology of the commercial Pt/C cathode material

4.2 MEA (Membrane Electrode Assembly) Preparation

The membrane electrode assembly is made of anode, Nafion 117 membrane and Fe-CNT-PA catalyst coated cathode electrode. Anode is commercial 10% Pt loaded carbon paper (Fuel Cell Earth). Cathode site is prepared by drop casting method and the

amount of the catalyst is 8 mg/cm^2. As depicted Figure 4-7, the first step of the MEA is the drop coating of the catalyst on the cathode electrode. Secondly, stacked anode, Nafion and cathode press at hot press at 130^{o}C, 0.4 ton/cm^2.

Figure 4-7 MEA assembly

After coating of the catalyst, it can be observed the thickness of the cathode electrode increases approximately 100% of the original thickness of the cathode. From the analysis of the modeling charge transfer in porous electrode, cathode reactions are kinetic limited reactions and also limited by electron and proton conduction sides which are at different phases (solid and electrolyte) potentials do change transfer through the cathode. In general, proton conduction limitation can be seen mostly toward at the end of the current collector side or at the beginning of the membrane. This is emphasize the

most important part of the electron flow entering the cathode has to be also conductive across the whole cathode layer before they can react with species (oxygen and protons). Therefore, the thickness of the catalyst layer is one of the critical parameters at the fuel cell experiment.

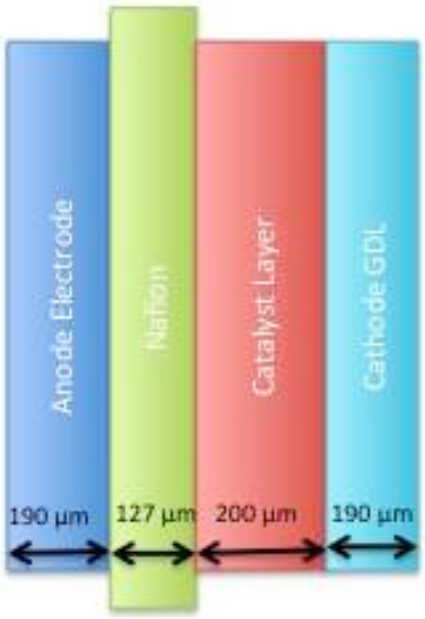

Figure 4-8 MEA the thickness of the electrodes and Nafion.

4.2.1 Nafion Pretreatment for the MEA

Commercial Nafion 115 membrane that's thickness is 127 micrometers needs pretreatment for functionalism the membrane itself. There are several steps at Nafion pretreatment processes. As depicted Figure 4-9, first Nafion membrane put in the 5% H_2SO_4 solution for 1 hour at 80^{o}C(a). Then it washes with DI water and boils it at DI

water and 5% H_2SO_4 at 80°C, respectively (b-d). Later, wash it with DI water (e). After boiling the membrane in DL water for 1 hour, store it in the glass jar with DI water (f).

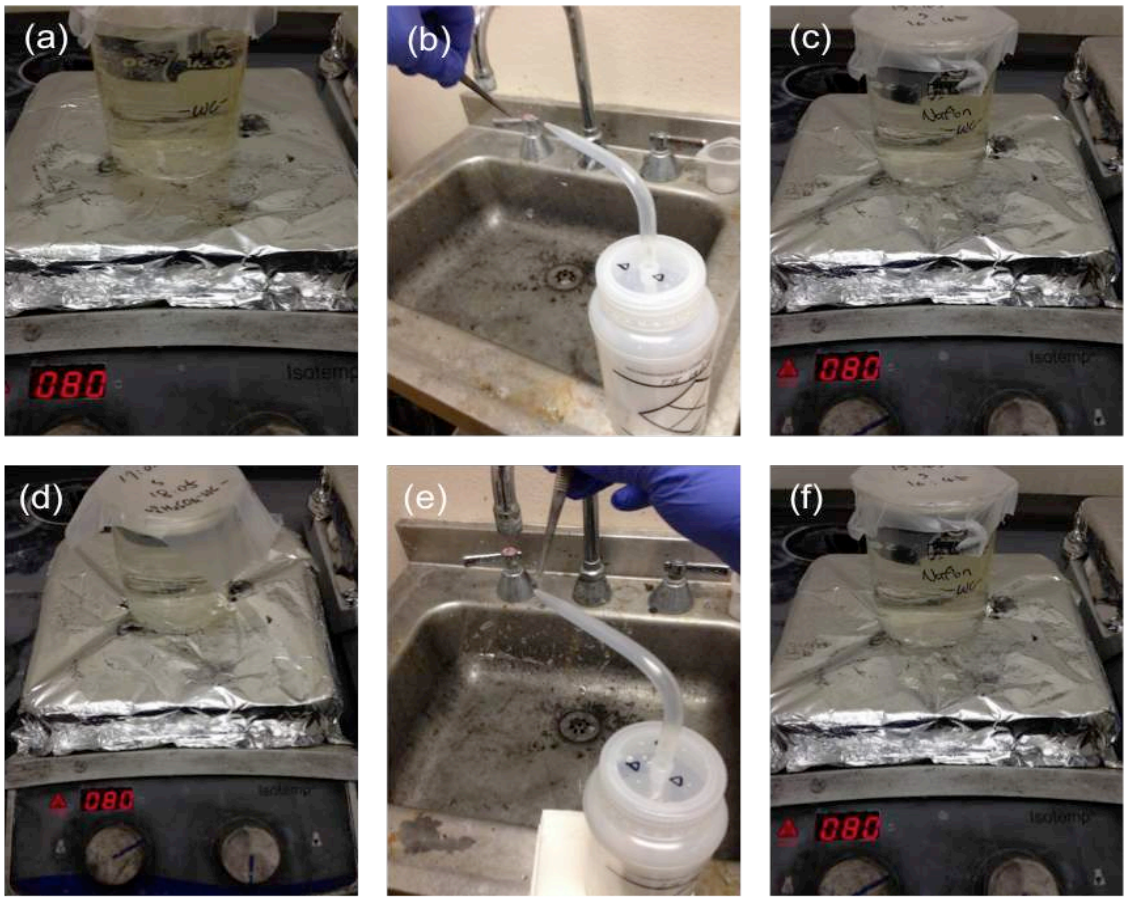

Figure 4-9 Nafion 117 pretreatment steps

4.3 Fuel Cell Test System

This section explains the experimental system of the PEM fuel cell. A PEM fuel cell is a sandwiched type of structure that is polymer membrane between anode and cathode catalyst layers. Bipolar plates are connected to the cell to form the fuel cell stack for the testing the system. The bipolar plates are designed to provide the gas flow channels on both sides of the plates. Moreover, it is used to electron transfer between MEA and end plates. It is also advancing the mechanical properties of the fuel cell. The flow channels are designed to remove the excessive amount of the water to avoid flooding that may block the gas flow. Also, bipolar plates should provide enough hydration for proton transfer between anode to cathode. End plates are the electrical connection surfaces between bipolar plates to external circuit.

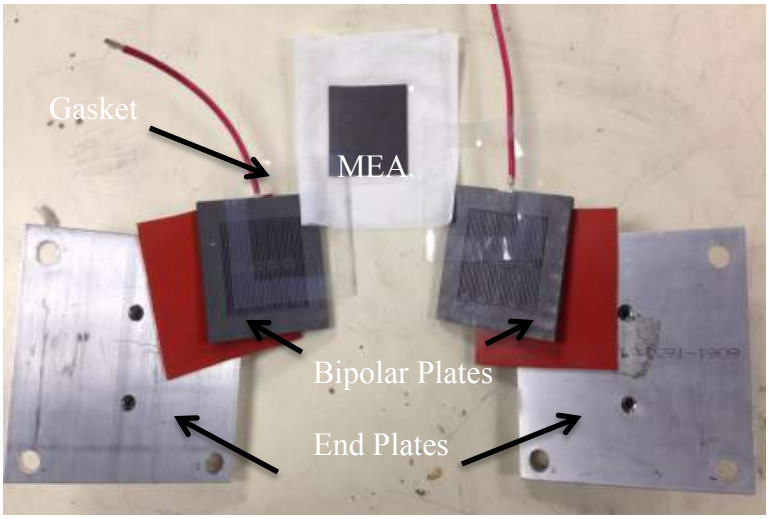

Figure 4-10 MEA and PEM fuel cell configuration

A schematic illustration of the fuel cell is shown in Figure 4-11. The system is made of a single fuel cell, two bubblers and flow meters, gas cylinders (hydrogen and oxygen). Heater and the thermocouple (TC) use for keep the temperature of the fuel cell constant at 80^{o}C through the fuel cell.

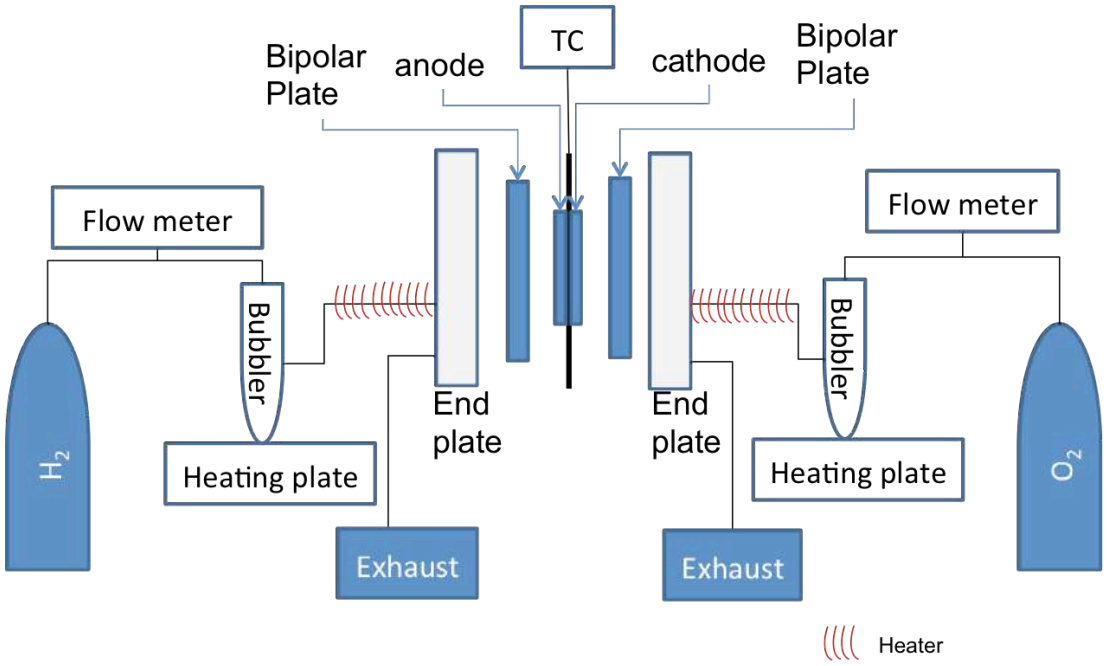

Figure 4-11 Schematic illustration of the fuel cell test system

Table 1 Parameter of the fuel cell test system

Catalyst layer	Temp.	(℃)	Pressure	(Bar)
Fe-CNT-PA	Tubing & cell temp. (℃)	80	Cathode pressure (bar)	2.8
Pt/C	Hydrogen (cc/min)	200	Anode pressure (bar)	2.8
	Oxygen (cc/min)	600		

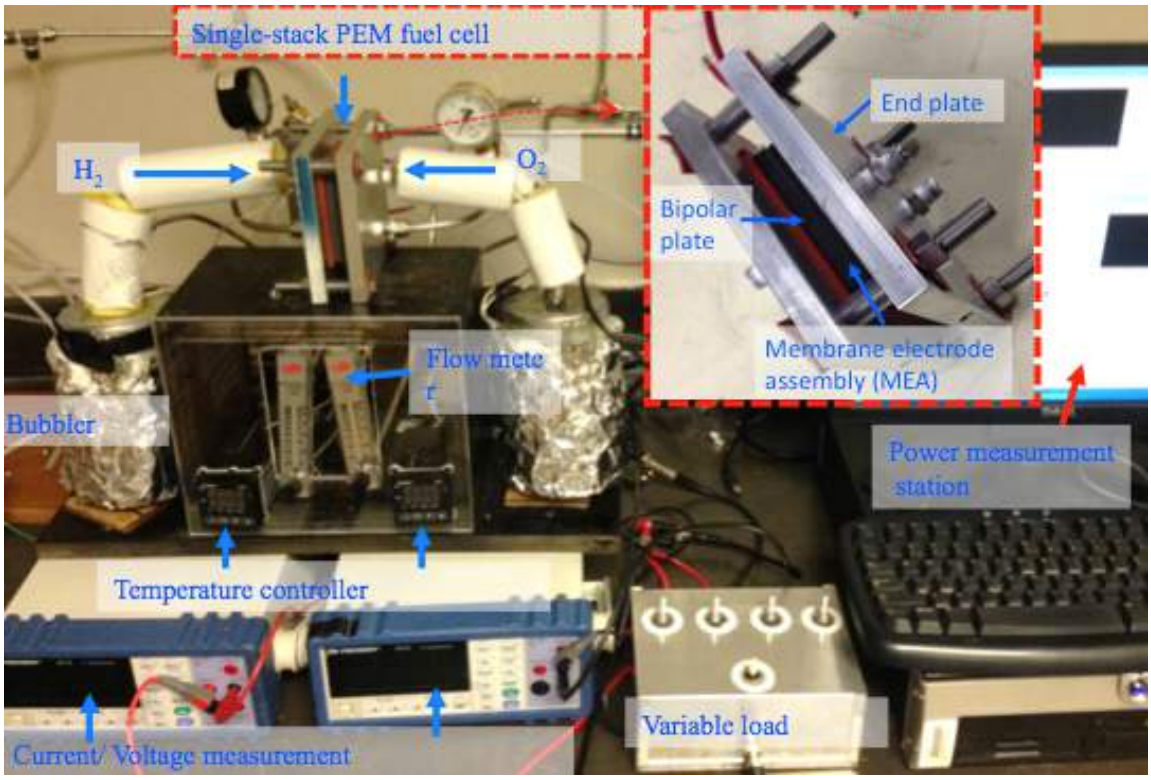

Figure 4-12 Single-stack PEM fuel cell test system

5 RESULTS AND DISCUSSION

In this chapter, experimental results are illustrated. Firstly, the electrochemical test results are explained, and then fuel cell measurements are investigated.

5.1 Electrochemical Test Results

Cyclic voltammetry tests are done with same amount (5 mg/cm^2) of Pt/C and Fe-CNT-PA catalysts on the carbon papers surface. Figure 5-1 is depicted there is a big peak density of current of the catalyst which illustrates high surface area of the catalyst and advancing transportation of the oxygen through the catalyst layer compare the commercial catalyst.

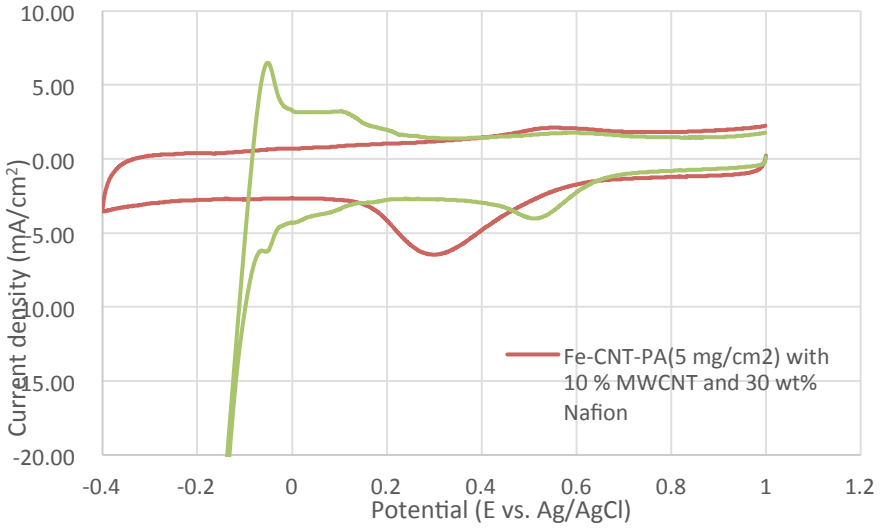

Figure 5-1 Cyclic voltammetry performances in 0.5 mole H_2SO_4

The catalytic activity of Fe-CNT-PA was tested with various compositions, which affect the electrical conductivity of the sample. Sample tested in 0.5 M H_2SO_4 electrolyte with 100sccm O_2 flow. From the figure 5-2, the performance of the Fe-CNT-PA with 10% wt of multi wall carbon nanotubes (MWCNT) was found the best in acidic ambient. At lower densities of current, kinetics of the electrons is dominated and at the higher current densities mass transfer is dominated.

At the kinetic dominated region, pure region is corresponded to the linear area of the Tafel plot. Due to high kinetic affect bulk solution mass transport has no influence at the current. The current, which is one sixth of the total current at the plot, is low according to several of researches[46].At the mass transport dominated region, current will be increase with the rotation rate.

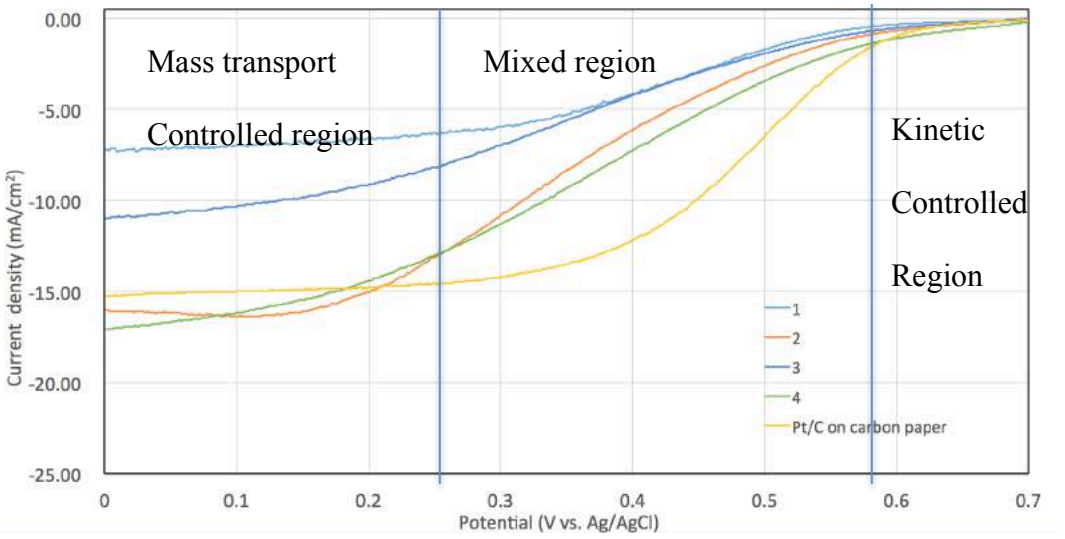

Figure 5-2 ORR performance of the samples above in 0.5 M H2SO4 at 1600 rpm

Table 2 Elemental composition of the Fe-CNT-PA and Pt/C catalyst for RDE test

Sample name	Loading weight (mg/cm^2)	Fe-CNT-PA (wt%)	Nafion (wt%)	Carbon black (wt%)	MWCNT (wt%)
1	5	60	30	10	-
2	5	70	20	-	10
3	5	60	30	-	10
4	8.3	60	30	-	10

The proposed Fe-CNT-PA catalyst tested at a homemade fuel cell testing system. Pure H_2 and O_2 gases were used without any part of humidification. The fuel cell voltage (V)/ current density curves have been taken at temperature at 80^oC. Pt/C catalyst (0.5 $mg_{Pt}cm^{-2}$) use for the comparison at cathode; both sides of the fuel cell's gas pressure are 2.8 bar. All tests used the commercial Pt/C anode that is loaded 0.5 $mg_{Pt}cm^{-2}$.

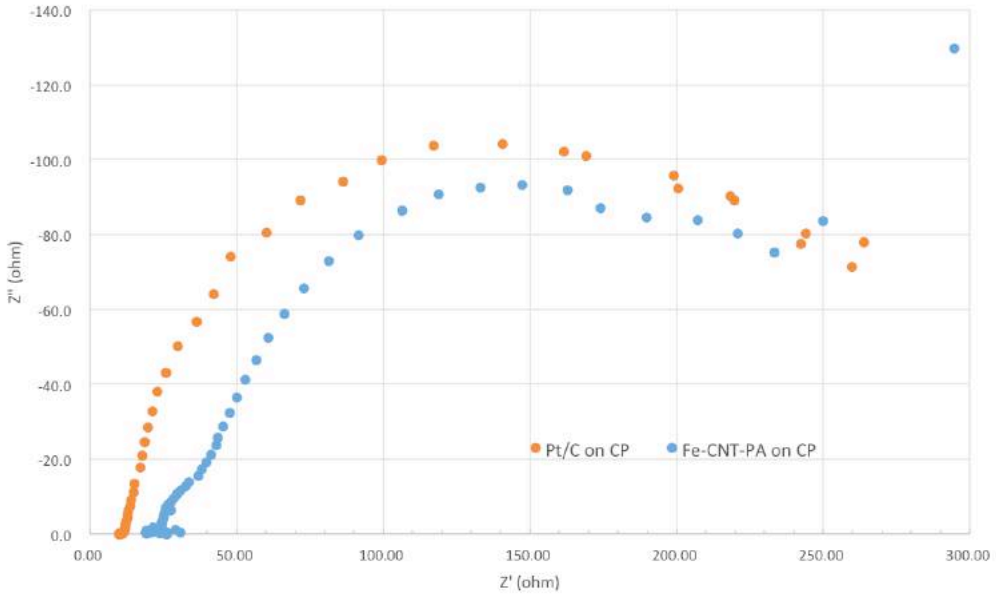

Figure 5-3 The EIS spectrum at of the catalyst coated fuel cell equivalent circuit in the Nyquist form. The angular frequency varies from 0.07 to $5x10^5$ rad/s.

Figure 5-3 illustrated the Nyquist form of the impedance spectra; the real impedance versus imaginary impedance part is shown at the figure. It shows the alternative current response at the angular frequency varies from 0.07 to $5x10^5$ rad/s. The beginning of the semi-circle is the ohmic resistance release on the x-axis at higher frequency ranges. The diameter of the semi-circle illustrates the charge transfer resistance, which is related to kinetics of the reaction. From the plot, starting point of the high frequency for Pt/C catalyst is 9 ohm and for the Fe-CNT-PA is 26 ohm. The diameter of the semi-circles of Pt/C and Fe-CNT-PA are 104 ohm and 93 ohm, respectively. From these results, it is clear the porous structure of the Fe-CNT-PA is advancing the reaction kinetic. On the other hand it has a big ohmic resistance due to its thickness of the catalyst layer.

5.2 Fuel Cell Test Results

Fuel cell polarization plot for Fe-CNT-PA catalyst and PANI-delivered catalysts, whose loading weight are 8 and 4 mg/cm^2 for comparison are illustrated in Fig 5-4. The best performance reaches with PANI-FeCo-C, which is mixed metal catalyst[23].

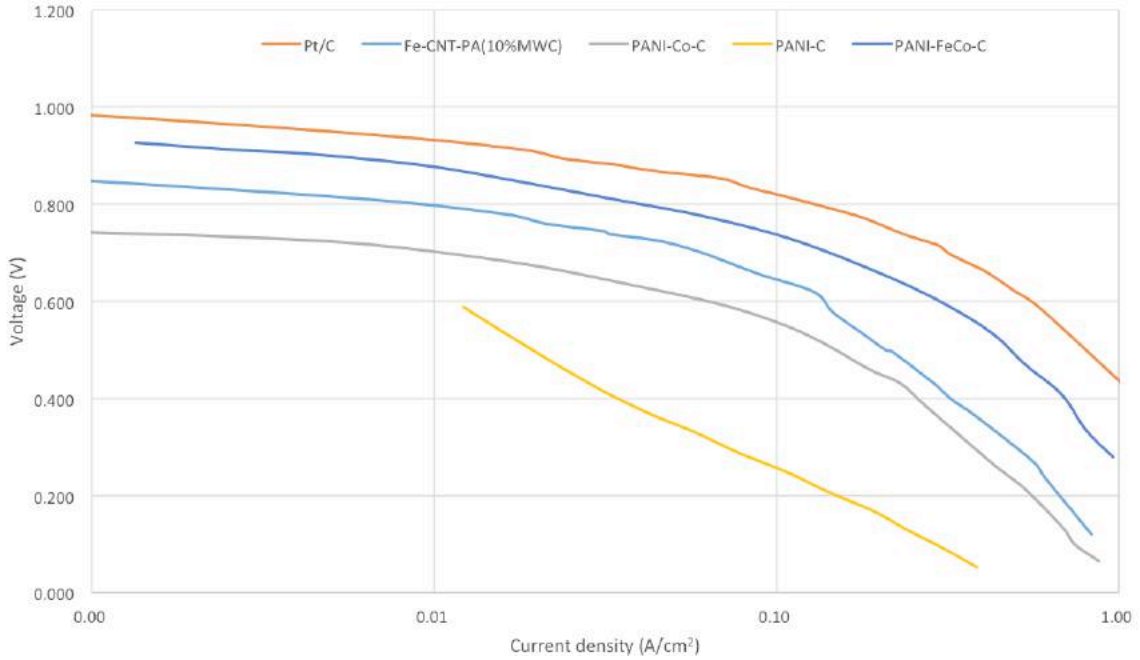

Figure 5-4 I/V curves at 80^{O}C for the fuel cell where the red line is commercial Pt/C, the blue line is Fe-CNT-PA with MWC that is compared with Science, 2011. 332**(6028): p. 443-447 [23] the dark blue line is PANI-FeCo-C, the yellow line is PANI-C and the grey line is PANI-Co-C.**

Overall performance of the non-precious catalyst is low compared the commercial Pt/C. From the results of the fuel cell, Fe-CNT-PA catalyst reaches the activity of state-of-art as Pt/C catalyst cathode side. However, its performance at lower potential is lower. This is caused by several reasons:

I. Catalyst ink preparation, architecture and coating have not been optimized. From the optical microscopes images, surface cracks are obvious on the coated side of the cathode electrode. It causes different activity of the catalyst that affect the performance[47, 48].

These problems can be solved in several ways;

a) Using a better coating method or better instruments to load the catalyst on the cathode surface.
b) Preparation of the catalyst can be reconsider to increase catalyst activity.
c) Improving the species transport characteristic of the Fe-CNT-PA catalyst.

6 CONCLUSION AND RECOMMENDATIONS

In this study, the catalytic activity of the Fe-CNT-PA catalyst is investigated through several electrochemical tests and with fuel cell experiments. While preparing the MEA for the fuel cell test, several coating methods are also investigated to find most suitable one for our case. Drop casting is chosen as coating methods due to coating by it is more easer and faster than all of aforementioned methods (rolling, dipping, syringe, spray gun). Each steps of the MEA preparation and assembly it to fuel is clearly defined at this thesis. Experimental part of this thesis has targeted testing the Fe-CNT-PA rather than synthesis the catalyst itself. Electrochemical results indicate it is a promising catalyst for ORR due its porous structure, but the process has to advancing to increase the activity of the catalyst. By increasing the kinetic activity of the catalyst, less catalyst ink may use to coat it on the top of the carbon paper, which causes thinner layer and less resistance.

Further study should be dedicated to advancing the coating method and increasing the activity of the catalyst by advancing the architectural structure of the catalyst. It is a promising catalyst is not only for PEM fuel cell but lots of other fuel cells and battery application.

REFERENCES

1. Information, N.N.C.f.E. *State of the Climate: Global Analysis for September 2015*. 2015 September 2015; Available from: http://go.nature.com/ZAEmAf.
2. Gielen, D., F. Boshell, and D. Saygin, *Climate and energy challenges for materials science.* Nature Materials, 2016. **15**(2): p. 117-120.
3. Rogelj, J. *The Emission Gap Report 2015*. 2015 [cited 2016; Available from: http://uneplive.unep.org/media/docs/theme/13/EGR_2015_301115_lores.pdf.
4. Schiermeier, Q., et al., *Electricity without carbon.* Nature, 2008. **454**(7206): p. 816-823.
5. *Key World Energy Statistics* 2015 [cited 2016; Available from: http:// www.iea.org.
6. Bruce, P.G., et al., *Li-O2 and Li-S batteries with high energy storage.* Nature materials, 2012. **11**(1): p. 19-29.
7. Vielstich, W., A. Lamm, and H.A. Gasteiger, *Handbook of fuel cells: fundamentals, technology, and applications*. Vol. 5. 2009: John Wiley & Sons.
8. Grove, W.R., *XXIV. On voltaic series and the combination of gases by platinum.* The London and Edinburgh philosophical magazine and journal of science, 1839. **14**(86): p. 127-130.
9. Nadal, M. and F. Barbir, *Development of a hybrid fuel cell/battery powered electric vehicle.* International journal of hydrogen energy, 1996. **21**(6): p. 497-505.

10. Wright, P.V., *Polymer electrolytes—the early days.* Electrochimica Acta, 1998. **43**(10): p. 1137-1143.

11. Barton, S.A.C., et al., *A methanol sensor for portable direct methanol fuel cells.* Journal of the electrochemical society, 1998. **145**(11): p. 3783-3788.

12. Yuh, C., et al., *Status of carbonate fuel cell materials.* Journal of power sources, 1995. **56**(1): p. 1-10.

13. Wagner, F.T., B. Lakshmanan, and M.F. Mathias, *Electrochemistry and the future of the automobile.* J. Phys. Chem. Lett, 2010. **1**(14): p. 2204-2219.

14. Strmcnik, D., et al., *Enhanced electrocatalysis of the oxygen reduction reaction based on patterning of platinum surfaces with cyanide.* Nature chemistry, 2010. **2**(10): p. 880-885.

15. Kalinoski, B.J.J. *DOE-EERE Fuel Cell Technologies Program-2009 DOE Hydrogen Program Review*. 2009 [cited 2016; Available from: www.hydrogen.energy.gov/pdfs/review09/fc_30_james.pdf.

16. J. Sinha, S.L.a.Y.Y. *DOE-EERE Fuel Cell Technologies Program DOE Hydrogen Program Review*. 2009 [cited 2016; Available from: www.hydrogen.energy.gov/pdfs/review09/fc_31_sinha.pdf.

17. Bell, A.T., *The impact of nanoscience on heterogeneous catalysis.* Science, 2003. **299**(5613): p. 1688-1691.

18. Li, Y. and G.A. Somorjai, *Nanoscale advances in catalysis and energy applications.* Nano letters, 2010. **10**(7): p. 2289-2295.

19. Zaera, F., *New challenges in heterogeneous catalysis for the 21st century.* Catalysis letters, 2012. **142**(5): p. 501-516.

20. Bezerra, C.W., et al., *A review of Fe–N/C and Co–N/C catalysts for the oxygen reduction reaction.* Electrochimica Acta, 2008. **53**(15): p. 4937-4951.

21. Hu, Y., et al., *Hollow spheres of iron carbide nanoparticles encased in graphitic layers as oxygen reduction catalysts.* Angewandte Chemie International Edition, 2014. **53**(14): p. 3675-3679.

22. Li, Y., et al., *An oxygen reduction electrocatalyst based on carbon nanotube-graphene complexes.* Nature nanotechnology, 2012. **7**(6): p. 394-400.

23. Wu, G., et al., *High-performance electrocatalysts for oxygen reduction derived from polyaniline, iron, and cobalt.* Science, 2011. **332**(6028): p. 443-447.

24. Herranz, J., et al., *Unveiling N-protonation and anion-binding effects on Fe/N/C catalysts for O2 reduction in proton-exchange-membrane fuel cells.* The Journal of Physical Chemistry C, 2011. **115**(32): p. 16087-16097.

25. Lefèvre, M., et al., *Iron-based catalysts with improved oxygen reduction activity in polymer electrolyte fuel cells.* science, 2009. **324**(5923): p. 71-74.

26. Oh, H.-S. and H. Kim, *The role of transition metals in non-precious nitrogen-modified carbon-based electrocatalysts for oxygen reduction reaction.* Journal of Power Sources, 2012. **212**: p. 220-225.

27. Zhang, J., *PEM Fuel Cell Electrocatalysts and Catalyst Layers: Fundamentals and Applications*. 2008: Springer- Verlag London Ltd, Guildford, Surrey, UK.

28. Nørskov, J.K., et al., *Origin of the overpotential for oxygen reduction at a fuel-cell cathode.* The Journal of Physical Chemistry B, 2004. **108**(46): p. 17886-17892.

29. K. S. Lyons, M.T., W. Baker and J. Pietron, *Low- Platinum Catalysts for Oxygen Reduction at PEMFC Cathodes*. 2005. p. 823-827.

30. Knözinger, H. and K. Kochloefl, *Heterogeneous catalysis and solid catalysts.* Ullmann's Encyclopedia of Industrial Chemistry, 2005.

31. Stamenkovic, V., et al., *Changing the activity of electrocatalysts for oxygen reduction by tuning the surface electronic structure.* Angewandte Chemie, 2006. **118**(18): p. 2963-2967.

32. Tripković, V., et al., *The oxygen reduction reaction mechanism on Pt (111) from density functional theory calculations.* Electrochimica Acta, 2010. **55**(27): p. 7975-7981.

33. Jasinski, R., *A new fuel cell cathode catalyst.* Nature 1964. **201**: p. 1212 - 1213

34. Herranz, J., et al., *Step-by-step synthesis of non-noble metal electrocatalysts for O2 reduction under proton exchange membrane fuel cell conditions.* The Journal of Physical Chemistry C, 2007. **111**(51): p. 19033-19042.

35. Matter, P.H. and U.S. Ozkan, *Non-metal catalysts for dioxygen reduction in an acidic electrolyte.* Catalysis letters, 2006. **109**(3-4): p. 115-123.

36. Matter, P.H., L. Zhang, and U.S. Ozkan, *The role of nanostructure in nitrogen-containing carbon catalysts for the oxygen reduction reaction.* Journal of Catalysis, 2006. **239**(1): p. 83-96.

37. Maldonado, S. and K.J. Stevenson, *Direct preparation of carbon nanofiber electrodes via pyrolysis of iron (II) phthalocyanine: electrocatalytic aspects for oxygen reduction.* The Journal of Physical Chemistry B, 2004. **108**(31): p. 11375-11383.

38. Maldonado, S. and K.J. Stevenson, *Influence of nitrogen doping on oxygen reduction electrocatalysis at carbon nanofiber electrodes.* The Journal of Physical Chemistry B, 2005. **109**(10): p. 4707-4716.

39. Proietti, E., et al., *Iron-based cathode catalyst with enhanced power density in polymer electrolyte membrane fuel cells.* Nature communications, 2011. **2**: p. 416.

40. Liu, H., et al., *High-surface-area CoTMPP/C synthesized by ultrasonic spray pyrolysis for PEM fuel cell electrocatalysts.* Electrochimica acta, 2007. **52**(13): p. 4532-4538.

41. Nie, Y., L. Li, and Z. Wei, *Recent advancements in Pt and Pt-free catalysts for oxygen reduction reaction.* Chemical Society Reviews, 2015. **44**(8): p. 2168-2201.

42. Yang, G., et al., *Scalable synthesis of bi-functional high-performance carbon nanotube sponge catalysts and electrodes with optimum C–N–Fe coordination for oxygen reduction reaction.* Energy & Environmental Science, 2015. **8**(6): p. 1799-1807.

43. Yang, G., et al., *Scalable synthesis of bi-functional high-performance carbon nanotube sponge catalysts and electrodes with optimum C–N–Fe coordination for oxygen reduction reaction.* Energy & Environmental Science, 2015.

44. *Bio-Logic Science Instruments, Calculation of the Platinum's Active Surface*. 2012 2016 [cited 2016; Available from: http://www.bio-logic.info/assets/app%20notes/20101105%20-%20application%20note%2011.pdf.

45. *Measurement Techniques Knowledgebase*. [cited 2016; Available from: http://www.scribner.com/scribner-associates-support/knowledgebase.

46. W. Vielstich, H.A.G., and A. Lamm, *Handbook of Fuel Cells. Fundamentals Technology and Applications*. 2003: John Wiley & Sons Ltd.

47. Fenster, C., et al., *Single tungsten nanowires as pH sensitive electrodes.* Electrochemistry Communications, 2008. **10**(8): p. 1125-1128.

48. Kaempgen, M., et al., *Multifunctional carbon nanotube networks for fuel cells.* Applied Physics Letters, 2008. **92**(9): p. 094103.